

ARTICLE

# Topology Optimization of Finite Periodic Structures with Compliance and Frequency Criteria

Chuanqi Zhu\*

Mechanical Engineering, University of Sydney, Sydney, NSW, Australia

## ABSTRACT

Periodic structures effectively address challenges in manufacturing, transportation, and installation of large-scale systems by streamlining processes and enhancing transport, replacement, and assembly efficiency. This paper introduces a topology optimization method specifically for cantilever beam structures, to minimize structural flexibility and optimize frequency by determining the optimal material distribution under given loads and constraints. The study explores continuum periodic structures, examining the effects of material properties, optimization parameters, and boundary conditions on the outcomes. Various aspects of periodic optimization design, such as structural configuration, connections, and layout, are also investigated. Through the application of topology optimization using SolidWorks and Ansys, the experimental results validate the method's effectiveness in enhancing structural performance and material utilization. This research presents a systematic approach and highlights the practical potential of designing periodic structures.

**Keywords:** Topology optimization; Periodic structures; Compliance; Frequency; Finite element analysis; ANSYS

## 1. Introduction

Over the past twenty years, structural topology optimization has seen significant growth, with its applications extending into aerospace, automotive, and civil engineer-

ing<sup>[1]</sup>. The focus has evolved beyond just weight and stiffness considerations to encompass dynamics, fatigue, and noise. Traditional design methodologies, which often depend heavily on the experience of designers, tend to lack

### \*CORRESPONDING AUTHOR:

Chuanqi Zhu, Mechanical Engineering, University of Sydney, Sydney, NSW, Australia; Email: [czhu3305@163.com](mailto:czhu3305@163.com)

### ARTICLE INFO

Received: 2 August 2024 | Revised: 2 September 2024 | Accepted: 6 September 2024 | Published Online: 20 September 2024  
DOI: <https://doi.org/10.30564/jmmr.v7i1.7152>

### CITATION

Zhu, C., 2024. Topology Optimization of Finite Periodic Structures with Compliance and Frequency Criteria. Journal of Metallic Material Research. 7(1): 22-31. DOI: <https://doi.org/10.30564/jmmr.v7i1.7152>

### COPYRIGHT

Copyright © 2024 by the author(s). Published by Bilingual Publishing Group. This is an open access article under the Creative Commons Attribution-NonCommercial 4.0 International (CC BY-NC 4.0) License. (<https://creativecommons.org/licenses/by-nc/4.0/>).

standardized procedures and quantitative rigor, resulting in inefficiencies<sup>[2]</sup>. The advent of finite element theory, coupled with advancements in computer technology, has transformed structural analysis, leading to more scientific and precise designs<sup>[3]</sup>.

Structural optimization can be categorized into size, shape, and topology optimization<sup>[4]</sup>. Although size and shape optimization are well-established areas, topology optimization, which seeks to determine the optimal material distribution for properties such as stiffness or frequency, remains a complex and challenging field<sup>[5]</sup>. The implementation of topology optimization is further complicated by manufacturing difficulties, particularly when dealing with intricate designs<sup>[6]</sup>.

This paper delves into the topology optimization of periodic continuum structures, focusing on compliance and frequency criteria, and employs ANSYS for case analysis. It examines the influence of critical parameters on structural flexibility and frequency, applying the insights gained to the detailed design of a support frame.

## 2. Literature review

Since the introduction of homogenization theory and continuous density functions by Bendsoe<sup>[5, 7]</sup>, topology optimization has undergone significant advancements, addressing the limitations of traditional methods such as dependence on initial designs and the need for remeshing. Subsequent research by van Dijk<sup>[6]</sup> highlighted the level set method (LSM) for its ability to clearly define boundaries, although challenges like controlling the length scale remain. Sigmund<sup>[8]</sup> stressed the importance of establishing standardized benchmarks to assess different optimization techniques, while Osanov<sup>[9]</sup> discussed the integration of topology optimization with additive manufacturing, pointing out issues like grid dependence.

In advanced structural design, Xia<sup>[10]</sup> explored the efficiency of the Bidirectional Evolutionary Structural Optimization (BESO) method, particularly in microstructure design. Wu<sup>[11]</sup> provided a classification of multi-scale structural optimization methods, identifying potential compatibility and computational complexity challenges.

Several practical case studies have illustrated the real-world applications of topology optimization. Enhanced

BESO method by improving numerical stability and reducing grid dependency, which addressed some of the practical limitations of earlier implementations. Zhou<sup>[12]</sup> employed the level set method to minimize frequency response, demonstrating its effectiveness in dynamic applications. Additionally, Andreassen optimized MATLAB code to enhance computational efficiency, reflecting ongoing efforts to improve the practical performance of optimization tools.

In engineering design, the integration of topology optimization with feature fitting algorithms has increased design flexibility, allowing for more adaptable and efficient solutions. Applications such as using ANSYS for optimizing complex structures, including brackets for ROV simulators, showcase the versatility and impact of topology optimization in solving real-world engineering challenges<sup>[13]</sup>.

## 3. Topology optimization methods

Topology optimization research is primarily categorized into two main areas: Truss Topology Optimization, which includes structures such as trusses, rigid frames, and grids; and Continuum Topology Optimization, which focuses on solid and shell structures. Continuum optimization is particularly prominent due to its critical role in determining the optimal material configuration within a structure, such as the number, size, and placement of voids, to achieve specific objectives under given constraints.

A widely adopted approach in this domain is the variable density method, which simplifies the complex homogenization theory by employing artificially defined material densities to establish a relationship between density and material properties. This method, which uses the relative density of each element as a design variable, provides benefits such as a reduced number of design variables, simplified sensitivity analysis, and increased computational efficiency. Because of its effectiveness, the variable density method is widely implemented in commercial software like ANSYS and OptiStruct. However, challenges such as numerical instabilities, including grid dependencies and checkerboard patterns, can occur and are usually addressed using filtering techniques.

In practical applications, topology optimization is typically conducted under idealized conditions, such as high mesh quality and uniform material properties. However,

these assumptions often diverge from the complexities encountered in real-world engineering scenarios. Additionally, the optimization outcomes can be sensitive to numerical instabilities and are often based on single working conditions, which may not fully capture the intricacies of actual design situations. Therefore, these factors require careful consideration, and further validation and refinement are often necessary when transitioning from research to practical applications.

In the context of applying the density penalty method for structural topology optimization, the penalty factor  $p$  associated with intermediate density materials plays a crucial role. This parameter is essential for eliminating intermediate densities to achieve minimal compliance, thereby clarifying the structural topology and improving maneuverability. A higher value of  $p$  more effectively drives intermediate densities toward 0, theoretically leading to a more optimal solution. The optimization results is shown in **Figure 1**.

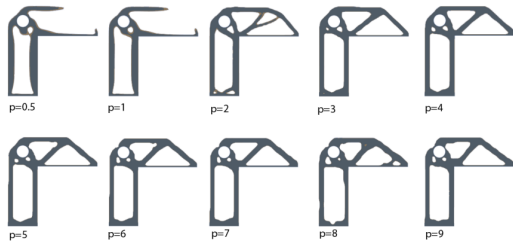


**Figure 1.** Optimization results for the different Penalty factor.

The optimization results indicate that when the penalty factor  $p$  ranges between 1 and 4, the topology remains stable, clearly delineating a well-defined force transmission path. However, as  $p$  exceeds 5, the topology undergoes significant changes, becoming more streamlined yet introducing a higher prevalence of intermediate densities. At  $p=1$ , the penalty function is linear and less effective at discouraging intermediate densities, resulting in less optimal material distribution. The most favorable results are generally observed with  $p$  values around 3 or 4, where there is an optimal balance between structural clarity and effective control over intermediate densities, leading to a well-defined and manufacture topology.

## 4. Variable density method

In the context of a two-dimensional static analysis problem, finite element theory is implemented by discretizing

the specified design domain into a finite number of elements. The principle of virtual work, which asserts that the total work performed by all active forces on a system's virtual displacements is zero, underpins the theoretical framework for finite element analysis. This principle is employed to derive equilibrium equations that enable the calculation of deformation, stress, and strain within complex structures. Specifically, for plane stress problems, the finite element equilibrium equations are formulated based on the principle of virtual work, providing a robust method for analyzing and solving such structural issues.

$$K \cdot U = F, \quad U = \frac{F}{K} \quad (1)$$

In finite element analysis, the equilibrium equation is expressed as  $F=KU$ , where  $F$  represents the nodal load vector,  $U$  denotes the nodal displacement vector, and  $K$  is the global stiffness matrix of the system, formed by assembling the stiffness matrices of all individual elements. This equation is fundamental in solving for the displacements at each node, which can then be used to determine the stress and strain distributions within the structure.

### 4.1 Principles of topology optimization

The isoparametric element framework employs two coordinate systems to enhance modeling flexibility: the actual coordinate system  $(x,y)$ , which represents the physical dimensions of elements like trapezoids, and the local coordinate system  $(\zeta,\eta)$ , used for simpler elements such as squares. This approach allows for an efficient representation of complex geometries by mapping the local coordinates to the actual coordinates through a transformation. This transformation involves defining a set of interpolation functions that link the local coordinates to the global system, ensuring that the element's shape, material properties, and response are accurately represented in the global model. By employing this transformation, the isoparametric element framework accommodates various element shapes and facilitates accurate numerical simulations, integrating local behaviors into a consistent global framework. This method is crucial for effectively analyzing complex structures and ensuring precise results in finite element analysis.

$$\begin{cases} x = \sum_{i=1}^4 N_i x_i \\ y = \sum_{i=1}^4 N_i y_i \end{cases} \quad (2)$$

$x_i$  and  $y_i$  are the coordinates of the element nodes,  $N_i$  is interpolation function.

When the element nodes are displaced, the displacement of any point inside the element can be expressed as:

$$\begin{cases} \frac{N_1}{4} = \frac{1}{4}(1-\zeta)(1-\eta) \\ \frac{N_2}{4} = \frac{1}{4}(1+\zeta)(1-\eta) \\ \frac{N_3}{4} = \frac{1}{4}(1-\zeta)(1+\eta) \\ \frac{N_4}{4} = \frac{1}{4}(1+\zeta)(1+\eta) \end{cases} \quad (3)$$

$$\begin{cases} u = \sum_{i=1}^4 N_i u_i \\ v = \sum_{i=1}^4 N_i v_i \end{cases} \quad (4)$$

Introducing a simple Jacobian matrix for single element analysis, the relationship between the strain within the element and the nodal displacements can be derived.

$$\{\epsilon\} = \begin{Bmatrix} \frac{\partial u}{\partial x} \\ \frac{\partial v}{\partial y} \\ \frac{\partial u}{\partial y} + \frac{\partial v}{\partial x} \end{Bmatrix} = \begin{bmatrix} \frac{\partial N_i}{\partial x} & 0 \\ 0 & \frac{\partial N_i}{\partial y} \\ \frac{\partial N_i}{\partial y} & \frac{\partial N_i}{\partial x} \end{bmatrix} \begin{Bmatrix} u_i \\ v_i \end{Bmatrix} = [B] \{\delta\} \quad (5)$$

In the context of finite element analysis, the geometric matrix [B] plays a crucial role in defining the mapping relationship between the natural coordinate system and the actual coordinate system of the element. This matrix essentially transforms coordinates from the natural system, which is often simpler and more convenient for theoretical derivation, to the actual system used in practical applications. Once the geometric matrix [B] is established, it allows for the derivation of the element stiffness matrix for plane problems. This derivation follows from applying the principle of virtual work, which involves calculating the work done by virtual forces and displacements to ensure that the stiffness matrix accurately represents the mechanical behavior of the element within the plane problem. The accuracy of the element stiffness matrix is essential for the reliable analysis and simulation of structural behavior.

$$K_e = t \int \int [B]^T [D] [B] |J| d\zeta d\eta \quad (6)$$

In this context,  $t$  represents the thickness of the element, which is a critical parameter in defining the element's response in structural analysis. The matrix ([D]) is the elasticity matrix, which characterizes the relationship between

stress and strain within the material. This matrix, often referred to as the constitutive matrix, encapsulates the material's mechanical properties, such as Young's modulus and Poisson's ratio, and is used to describe how the material deforms under applied stresses. By incorporating the thickness ( $t$ ) and the elasticity matrix ([D]), the analysis accurately models how the element behaves under various loading conditions, ensuring that the computed stresses and strains reflect the true mechanical response of the material.

## 4.2 Variable density method

The core concept of the variable density method is to assume the existence of a material element with a density that varies rather than being fixed. The structure is then discretized using the finite element method, with the density of each material element treated as a continuous variable ranging between 0 and 1. Furthermore, a functional relationship is assumed between the material density and its physical properties, enabling these properties to be expressed as functions of the element's density.

Using the global volume as a constraint and considering stiffness topology optimization for a continuum structure:

$$\begin{aligned} \rho &= \{\rho_1, \rho_2, \rho_3, \dots, \rho_n\}^T \in \Omega \\ 0 < \rho_{min} \leq \rho_i \leq 1 \quad (i = 1, 2, 3, \dots, n) \\ C(x) &= F^T U \quad v^* \leq fV \end{aligned} \quad (7)$$

By introducing variable density materials, the originally discrete topology optimization problem is converted into a continuous one, making it more tractable. However, this approach often leads to a substantial number of elements with intermediate densities, which are impractical for manufacturing.

To mitigate this issue, a material interpolation model with an intermediate density penalty function is proposed. This model effectively reduces the occurrence of intermediate densities, steering the material densities in the optimized design towards either 0 or 1, thus yielding results that are more practical and manufacturable.

In variable density methods, interpolation models include the Solid Isotropic Material with Penalization (SIMP) model and the Rational Approximation of Material Properties (RAMP) model. In the SIMP interpolation model, the elastic modulus of the element is expressed as: where  $(E_e)$  is the elastic modulus of the element,  $(E_0)$  is the elastic

modulus of the material, and  $(\rho_e)$  is the relative density of the element. To avoid numerical singularities in finite element calculations, a lower limit of  $(\rho_n = 10^{-3})$  is typically used;  $(P)$  is the penalty factor, and  $(p = 3)$  is usually chosen to minimize compliance in the optimization problem. These conclusions and their clear representation are illustrated in the following **Figure 2**, as discussed in my earlier optimization experiments.

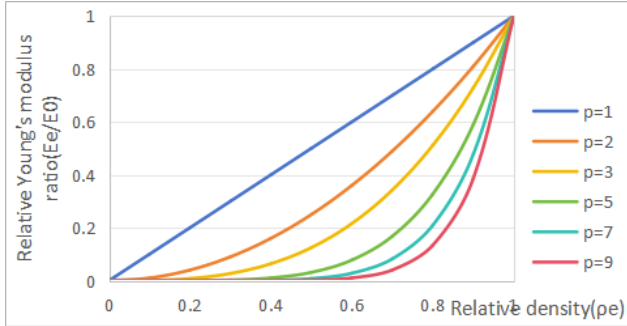


**Figure 2.** Solid Isotropic Material with Penalization model.

As illustrated in **Figure 2**, the specific stiffness, given by  $E/\rho$ , behaves differently depending on the penalty factor  $p$ . For intermediate density values from 0 to 1, the specific stiffness is higher when the penalty factor  $p$  is set to 1. In contrast, when  $p$  is greater than 1, the specific stiffness decreases. The design variable  $\rho$  ranges from 0 to 1, affecting the relationship between stiffness and density. This characteristic pushes the design variable towards the extremes—either 0 or 1—resulting in the SIMP (Solid Isotropic Material with Penalization) interpolation model tending to produce binary (0/1) design outcomes.

The core feature of the SIMP model is its penalized interpolation process, which promotes this binary distribution. In an improved model, the lower bound of the density variable can be set to 0. The mathematical expression for this is:

$$E_e = E_m + (E_0 - E_m)\rho_e^p \quad (8)$$

### 4.3 Sensitivity analysis

In structural optimization, sensitivity analysis plays a crucial role in updating design variables. This process involves computing the derivatives of the objective and constraint functions with respect to the design variables. The load vector, which is constant and independent of the design

variables, functions as an input condition in this analysis.

$$\frac{\partial F}{\partial x_i} = 0 \quad (9)$$

$$\frac{\partial v^*}{\partial x_i} = \sum_{i=1}^n v_i \quad (10)$$

The compliance formula for the SIMP model expressed as follows:

$$C = F^T U \quad (11)$$

$$C = F^T U + \lambda^T (KU - F) \quad (12)$$

The partial derivative of  $\rho_e$  on both sides of the formula represents the sensitivity of the objective function with respect to changes in the element density. This derivative is crucial for updating the design variables during the optimization process, guiding the material distribution toward an optimal solution.

$$\frac{\partial C}{\partial \rho_e} = (F^T + \lambda^T K) \frac{\partial U}{\partial \rho_e} + \left( \frac{\partial F^T}{\partial \rho_e} U - \lambda^T \frac{\partial F}{\partial \rho_e} \right) + \lambda^T \frac{\partial K}{\partial \rho_e} U \quad (13)$$

The Stiffness formula is

$$F = K \cdot U \quad (14)$$

The compliance sensitivity analysis expression is designed to be self-adjoint and incorporates the displacement vector. This means that the analysis takes into account how changes in the displacement vector influence compliance, and it inherently maintains a symmetrical relationship. This self-adjoint property simplifies the analysis and ensures that the sensitivity calculations are consistent and reliable, reflecting the impact of displacement variations on the overall compliance. This means that the expression can be symmetrically expressed in terms of the design variables, further emphasizing the direct relationship between the structure's response and the design modifications. This relationship can be expressed as a concise function of the design variables and their corresponding sensitivities.

$$\frac{\partial C}{\partial \rho_e} = -u_e^T \frac{\partial k_e}{\partial \rho_e} u_e \quad (15)$$

$$\rho_e = \frac{\rho_i}{\rho_0}, E_i = E_0 \rho_e^p, v_i = v_0 \quad (16)$$

This sensitivity measure provides insight into how variations in the density of individual elements impact the overall

compliance of the structure, serving as a crucial metric in guiding the optimization process toward more efficient material distribution.

$$\alpha_i^e = \frac{\partial C}{\partial \rho_e} = \rho_e^{p-1} \{u_i^e\}^T [K_i^e] \{u_i^e\} \quad (17)$$

The structure's dynamic behavior can be represented by an eigenvalue problem, with the equation for undamped free vibration being

$$K\Phi_j = \omega_j^2 M\Phi_j \quad (18)$$

The partial derivative with respect to  $\rho_e$  is:

$$\frac{\partial \omega_j^2}{\partial \rho_e} = \Phi_j^T \frac{\partial K}{\partial \rho_e} \Phi_j - \Phi_j^T \omega_j^2 \frac{\partial M}{\partial \rho_e} \Phi_j \quad (19)$$

### 5. ANSYS workbench

In topology optimization, the initial structure is discretized into a finite element mesh, with boundary and loading conditions applied to simulate real-world operating conditions. The structure is optimized based on specific objectives

and constraints, producing a new topological configuration. This configuration undergoes further finite element analysis and evaluation until the design criteria are met.

For the topology optimization of a cantilever beam, Ansys is used to model and analyze a bridge structure measuring 50m in length, 10m in width, and 7m in height. Fixed constraints are applied at both ends, and a pressure of 100 MPa is applied to the bridge deck. The structure is discretized with a rectangular mesh, and static analysis is performed to determine stress and displacement distributions, as shown in **Figure 3**. The optimization process aims to reduce the structure's volume to 35% while maximizing stiffness. Key steps involve setting optimization parameters, defining non-optimized regions (such as support structures), and establishing a minimum volume constraint. After 18 iterations, the bridge volume is reduced by 63.3%, with corresponding changes in displacement and stress distribution, as shown in **Figure 4**. Post-processing is then carried out to standardize the optimized structure for manufacturing.

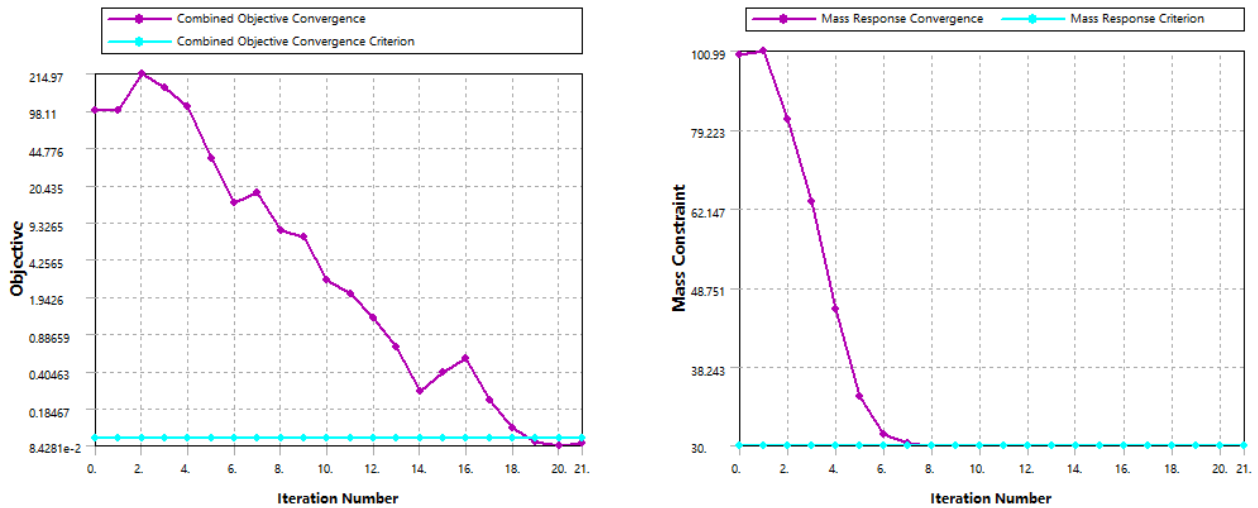


Figure 3. Optimization iteration number and volume response convergence relationship curve.

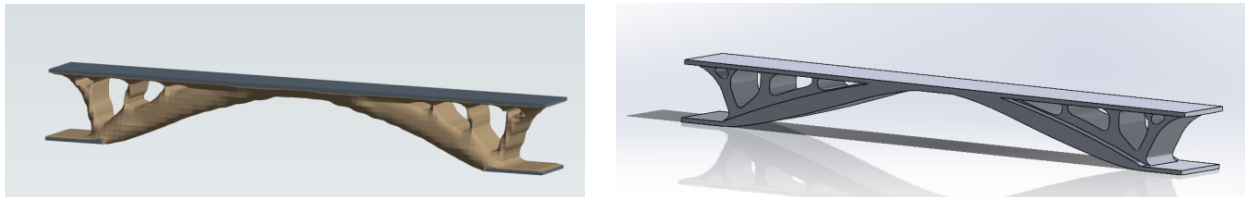


Figure 4. Bridge post-processing results (left); Bridge post-processing results (right).

Through the optimization process, the bridge's volume and mass were reduced by 58.2%, from 3,500 cubic meters to 1,463 cubic meters, while maintaining structural integrity. The maximum displacement increased by 512%, reflecting greater flexibility, though still within acceptable limits. The average stress rose by 306% to 22.4 MPa, with the maximum stress increasing slightly from 121 MPa to 210 MPa, which remains within the strength requirements for concrete.

Post-optimization modal analysis revealed notable improvements in the bridge's vibration characteristics. The first-order frequency decreased from 14.6 Hz to 5.8 Hz, indicating better overall vibration performance. While the second-order mode saw a smaller reduction, the third-order mode improved significantly, decreasing by 61%. The maximum deformation shifted to the sixth mode, with a value of 0.0012 m.

## 6. Periodic structure

In the design of periodic structures, symmetry plays a vital role due to its significant influence on alignment, assembly, and the overall performance of the structure. Symmetry facilitates the installation process by ensuring proper orientation and alignment of components, which is critical for preserving structural integrity.

### 6.1 Structural symmetry

This study uses a brick-shaped object with dimensions of 2 meters in length and 1 meter in height as the analysis model. The left side of the brick is fixed, while the right side is subjected to three forces of 500 N each, simulating the load on periodically arranged structures. The model employs a grid size of 0.025 meters, resulting in 9,830 nodes. Flexibility and frequency were chosen as the optimization targets, with a requirement that the structure's volume increase by at least 40% over the original to ensure quality. Asymmetric results of this optimization process are shown in **Figure 5**.

The original structure exhibited a maximum stress of approximately 0.61 MPa and a maximum deformation around 0.0007 mm. The displacement influenced by frequency varied between roughly 0.36 mm and 0.56 mm. The effects of different symmetry constraints on the structure are presented in **Figure 6**.

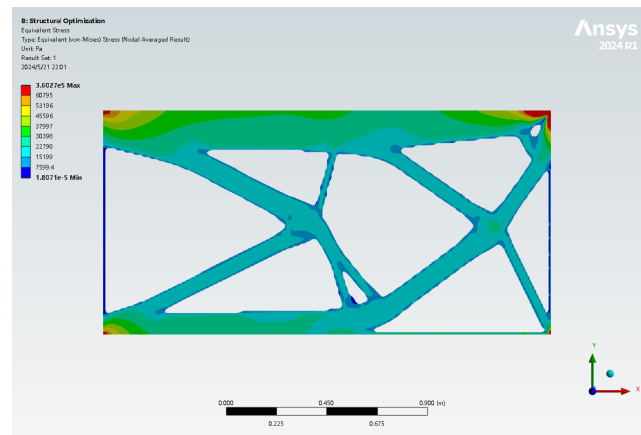


Figure 5. Asymmetric results.

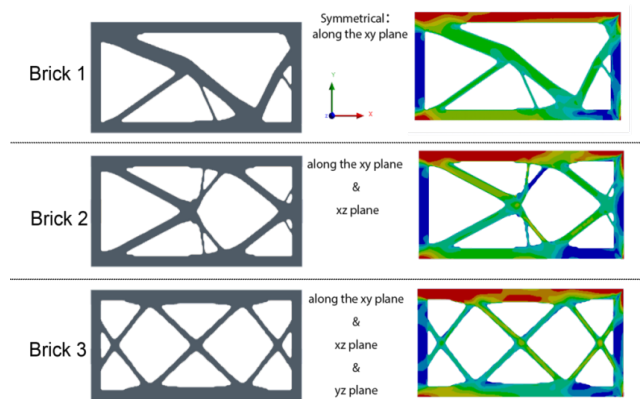


Figure 6. Different symmetry constraint results.

Topology optimization is used to efficiently allocate materials within specific constraints, aiming to achieve optimal performance. For example, Brick1 demonstrated superior performance under minimal topology optimization constraints, suggesting that fewer constraints allow the design to better utilize material properties, thereby enhancing structural effectiveness. However, one significant drawback of Brick1 is its stringent installation requirements, which limit its adaptability to different operational conditions. Although its performance is excellent, these strict installation demands could present challenges in real-world applications.

In contrast, Brick2 and Brick3 incorporate symmetry constraints in their design. While symmetry can simplify manufacturing and installation processes, it may also lead to some performance trade-offs. Specifically, the symmetry requirement in Brick2 and Brick3 can restrict the ability of certain materials to fully support and stabilize the structure under stress, resulting in a reduction in overall performance.

## 6.2 Arrange

The arrangement of periodic structural bricks requires careful consideration of optimal material distribution and structural performance, guided by constraints set through topology optimization. Various configurations were analyzed, including a fully symmetrical structure as well as uniaxially symmetrical structures. The fully symmetrical arrangement ensures uniform performance across all directions, while uniaxial symmetry introduces variations in stiffness and stability. The different arrangement methods are shown in **Figure 7**.

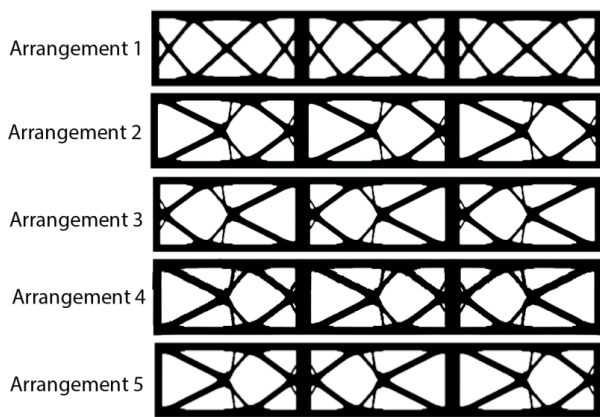


**Figure 7.** Arrangement method.

Among the analyzed configurations, the arrangement with a reversed alignment in the middle proved to be the weakest, showing the highest deformation and reduced stiffness. In contrast, the configuration aligned with the original topology optimization design demonstrated the highest structural stiffness and the smallest displacement, approximately 0.015 mm, highlighting its superior performance.

## 7. Experiment design

The support frame is a structural mechanism made up of multiple cantilever beams, designed for use in the structural units of large buildings. As depicted in **Figure 8**, the frame is constructed from aluminum alloy and has overall dimensions of approximately 700 mm by 750 mm by 1800 mm.

This frame consists of three columns, three width support beams, and four length support beams on one side. The columns measure around 100 mm by 100 mm by 750 mm,

the width support beams are about 100 mm by 50 mm by 500 mm, and the length support beams measure approximately 800 mm by 50 mm by 150 mm. The total weight of this side of the structure is roughly 149.6 kg. Before optimization, the cantilever beams on this side, which are the focus of the optimization, weighed about 87.1 kg. This side of the structure supports its own weight and is subjected to a pressure of 1 MPa applied to the mid-end support beam. The columns on this side of the frame are fixedly supported to accommodate the counterweight design.

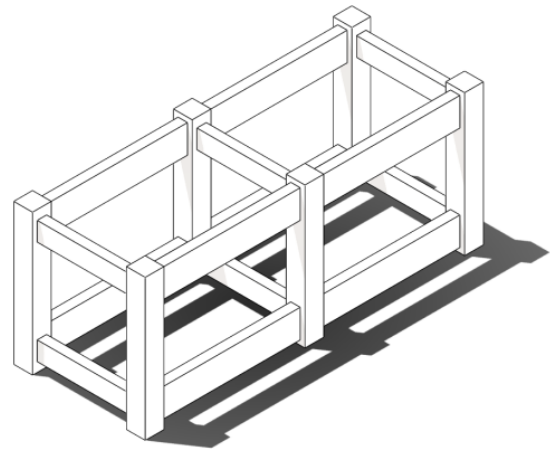


**Figure 8.** Support frame structure.

Support beam length is 500 mm but divided into two sections, each measuring approximately 243.8 mm in length. The volume of each support beam is around  $1.2187 \times 10^{-3} m^3$ , and the mass is about 3.376 kg. The maximum stress in the support frame is roughly 6.45 MPa, and the vertical displacement is approximately 0.0033 mm.

Over 60 iterations in ANSYS Workbench, the mass is reduced to 32.90% of the initial part, bringing it down to about 1.11 kg. The maximum stress increases to roughly 11.3 MPa, and the vertical displacement is around 0.0374 mm. Stress analysis results and the topology optimization structure can be seen in **Figure 9**.

The post-optimization model has a complex structure with uneven surfaces, which presents challenges for manufacturing. In the post-processing stage, the model is redesigned using standard features to correct these surface irregularities. Smoothing algorithms and tools like SpaceClaim or Blender software are applied to refine the mesh, achieving a more consistent surface height and reducing surface imperfections. Additionally, the geometry is simplified using standard ma-



chining features, which not only lowers manufacturing costs but also provides more practical machining solutions. Functional elements such as holes, smooth surfaces, and channels

are then incorporated according to the specific requirements. The final result of the width direction optimization is shown in **Figure 10**.

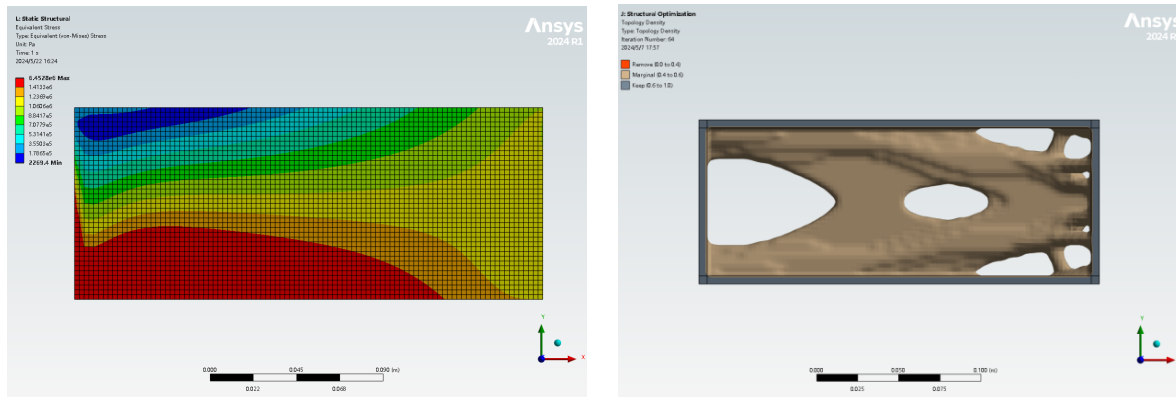


**Figure 9.** Stress analysis in ANSYS Workbench (left); Topology optimization structure in ANSYS Workbench (right).

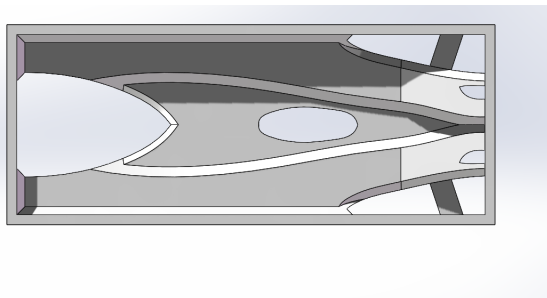


**Figure 10.** Width direction optimization final result.

## 8. Conclusion

This study successfully demonstrated the application of topology optimization in designing finite periodic structures, emphasizing both compliance and frequency criteria. By leveraging advanced techniques such as the variable density approach and employing sophisticated tools like ANSYS, the research achieved notable improvements in material distribution within cantilever beam structures. These enhancements led to substantial gains in structural performance and material efficiency, highlighting the efficacy of topology optimization in addressing complex engineering problems.

The findings of this study illustrate the substantial benefits of using topology optimization to create more robust and efficient structures while adhering to various constraints. The research not only showcases the technique’s potential in optimizing material usage but also in achieving superior structural integrity and functionality.

Looking ahead, future research could build on these findings by exploring the application of topology optimization in more intricate multi-physics scenarios. This could involve integrating additional factors such as thermal, fluid, or electrical effects, thereby broadening the scope and impact of this optimization approach. Such advancements would further extend the practical applications of topology optimization, offering even greater potential for innovation and efficiency in engineering design.

## Conflict of Interest

The author declares no conflicts of interest.

## Funding

This research received no external funding.

## Acknowledgments

I would like to express gratitude to Prof. Qing Li for his invaluable guidance and support throughout this research.

## References

- [1] Rozvany, G.I.N., 2001. A critical review of established methods of structural topology optimization. *Structural and Multidisciplinary Optimization*. 21(3), 164–184.
- [2] Qian, L., 2001. Optimal design of engineering struc-

- tures. In: Qian Xuesen's Technical Scientific Thoughts and Mechanics. pp. 47–50.
- [3] Lyu, Y., 2022. Finite element method: Element solutions. 1st ed. Springer. DOI: <https://doi.org/10.1007/978-981-19-3363-9>
- [4] Zuo, K., 2023. Research on the theory and application of continuum structural topology optimization [PhD thesis]. Huazhong University of Science and Technology.
- [5] Bendsøe, M.P., Kikuchi, N., 1988. Generating optimal topologies in structural design. *Computer Methods in Applied Mechanics and Engineering*. 71(2), 197–224.
- [6] van Dijk, N.P., Maute, K., Langelaar, M., et al., 2013. Level-set methods for structural topology optimization: A review. *Structural and Multidisciplinary Optimization*. 48(3), 437–472. DOI: <https://doi.org/10.1007/s00158-013-0912-y>
- [7] Bendsøe, M., Sigmund, O., 1999. Techniques for material interpolation in topology optimization. *Archive of Applied Mechanics*. 69(9–10), 635–654. DOI: <https://doi.org/10.1007/s004190050248>
- [8] Sigmund, O., Maute, K., 2013. Topology optimization approaches: A comparative review. *Structural and Multidisciplinary Optimization*. 48(6), 1031–1055. DOI: <https://doi.org/10.1007/s00158-013-0978-6>
- [9] Osanov, M., Guest, J.K., 2016. Topology optimization for architected materials design. *Annual Review of Materials Research*. 46(1), 211–233. DOI: <https://doi.org/10.1146/annurev-matsci-070115-031826>
- [10] Xia, L., Xia, Q., Huang, X., 2018. Bi-directional evolutionary structural optimization on advanced structures and materials: A comprehensive review. *Archives of Computational Methods in Engineering*. 25, 437–478. DOI: <https://doi.org/10.1007/s11831-016-9203-2>
- [11] Wu, J., Sigmund, O., Groen, J.P., 2021. Topology optimization of multi-scale structures: A review. *Structural and Multidisciplinary Optimization*. 63(3), 1455–1480. DOI: <https://doi.org/10.1007/s00158-021-02881-8>
- [12] Zhou, M., Fleury, R., Shyy, Y.K., Thomas, H., Brennan, J., 2002. Progress in topology optimization with manufacturing constraints. In 9th AIAA/ISSMO Symposium on Multidisciplinary Analysis and Optimization. p. 5614.
- [13] Sugiyama, M., Suzuki, T., Kanamori, T., 2012. Density-ratio matching under the bregman divergence: A unified framework of density-ratio estimation. *Annals of the Institute of Statistical Mathematics*. 64(5), 1009–1044.